JACS
JOURNAL OF THE AMERICAN CHEMICAL SOCIETY

ARTICLE

pubs.acs.org/JACS

Chemiluminescent and Chemiluminescence Resonance Energy Transfer (CRET) Detection of DNA, Metal Ions, and Aptamer−Substrate Complexes Using Hemin/G-Quadruplexes and CdSe/ZnS Quantum Dots

Ronit Freeman,[†] Xiaoqing Liu,[†] and Itamar Willner*

Institute of Chemistry, Center of Nanoscience and Nanotechnology, The Hebrew University of Jerusalem, Jerusalem 91904, Israel

ABSTRACT: Nucleic acid subunits consisting of fragments of the horseradish peroxidase (HRP)-mimicking DNAzyme and aptamer domains against ATP or sequences recognizing Hg^{2+} ions self-assemble, in the presence of ATP or Hg^{2+}, into the active hemin−G-quadruplex DNAzyme structure. The DNAzyme-generated chemiluminescence provides the optical readout for the sensing events. In addition, the DNAzyme-stimulated chemiluminescence resonance energy transfer (CRET) to CdSe/ZnS quantum dots (QDs) is implemented to develop aptamer or DNA sensing platforms. The self-assembly of the ATP-aptamer subunits/hemin-G-quadruplex DNAzyme, where one of the aptamer subunits is functionalized with CdSe/ZnS QDs, leads to the CRET signal. Also, the functionalization of QDs with a hairpin nucleic acid that includes the G-quadruplex sequence in a "caged" configuration is used to analyze DNA. The opening of the hairpin structure by the target DNA assembles the hemin−G-quadruplex DNAzyme that stimulates the CRET signal. By the application of three different sized QDs functionalized with different hairpins, the multiplexed analysis of three different DNA targets is demonstrated by the generation of three different CRET luminescence signals.

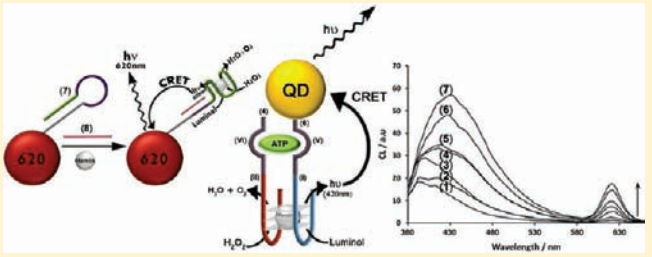

INTRODUCTION

The application of nucleic acids for the optical detection of DNA, aptamer−substrate complexes, or metal ions attracted substantial research efforts in the past decade. The color changes upon the aggregation of Au nanoparticles provided a versatile method to detect DNA,[1] aptamer−substrate recognition processes,[2−4] and metal ions[5−7] such as Hg^{2+}. Different fluorescent and fluorescence resonance energy transfer DNA sensors[8] and aptasensors[9−13] were developed. Similarly, semiconductor quantum dots (QDs) were used as luminescence labels for the detection of DNA[14,15] or as optical labels for following the dynamic replication and sensing of DNA,[16] or the dynamic formation of aptamer−substrate complexes.[17,18] Catalytic nucleic acids (DNAzymes) attract substantial research efforts as amplifying labels for sensing events.[19] Different ion-dependent DNAzymes have been implemented as catalysts for the optical detection of metal ions, such as Pb^{2+}, UO_2^{2+}, and Cu^{2+} through the cleavage of substrates modified with a fluorophore−quencher pair,[20−22] or by the catalytic deaggregation of Au nanoparticles.[23] One of the most extensively studied DNAzymes is the hemin/G-quadruplex horseradish peroxidase (HRP) mimicking DNAzyme,[24,25] that catalyzes the oxidation of 2,2′-azino-bis(3-ethylbenzthiazoline-6-sulfonic acid) $ABTS^{2-}$ by H_2O_2 to the colored product $ABTS^{\bullet-}$. This DNAzyme was used as a catalytic label for the colorimetric detection of DNA,[19] aptamer complexes,[26−29] and metal ions.[30,31] Recently, different DNA replication platforms that catalytically synthesize amplifying DNAzymes were used for the optical detection of DNA,[32] aptamer compelxes,[33,34] and metal ions.[7] The hemin/G-quadruplex was also found to quench the luminescence of semiconductor quantum dots via electron transfer. This function was implemented to develop different assays for the detection of DNA or aptamer-substrate complexes.[35] The hemin/G-quadruplex HRP mimicking DNAzyme was also found to act as a catalyst for the generation of chemiluminescence through the oxidation of luminol by H_2O_2. This was used to develop chemiluminescent DNA sensors.[36,37]

In the present study, we report on the development of chemiluminescent Hg^{2+} and adenosine-5′-triphosphate, ATP, sensors based on the Hg^{2+}- or ATP-induced self-assembly of nucleic acid subunits into the hemin/G-quadruplex catalytic label. This enables the chemiluminescent detection of the respective analytes. Most important in the present study is, however, the demonstration that the chemiluminescence, generated by the hemin/G-quadruplex, acts as an internal light source for the chemiluminescence resonance energy transfer (CRET) to CdSe/ZnS QDs. This process triggers-on the luminescence of the QDs. We introduce the CRET-based detection of ATP and DNA by the appropriate modification of QDs with nucleic acids capable of

Received: March 23, 2011
Published: June 16, 2011

assembling the hemin/G-quadruplex DNAzyme upon detecting different analytes. This technique allowed the application of differently sized QDs functionalized with different nucleic acids for the multiplexed CRET-based detection of different DNA targets.

EXPERIMENTAL SECTION

Materials and Reagents. Ultrapure water from a NANOpure Diamond (Barnstead Int., Dubuque, IA) source was used throughout the experiments. Hops Yellow Core Shell EviDots, CdSe/ZnS Quantum dots in toluene were purchased from Evident Technologies. *N*-[e-Maleimidocaproyloxy]succinimide ester (EMCS) was purchased from Pierce Biotechnologies. Stock solutions of 5 mM hemin and 250 mM luminol were prepared in DMSO and stored in the dark at −20 °C.

The DNA constructs were purchased from Sigma Life Science (U.K.). All oligonucleotides were HPLC-purified, and freeze-dried by the supplier. The oligonucleotides were used as provided and diluted in 10 mM Tris-HCl buffer solution, pH 8, to give a stock solution of 100 μM.

The sequences of the oligomers are as follows:

(**1**) 5′-TCGCTTGTGGAGGG-3′
(**2**) 5′-GGGACGGGTTGCGA-3′
(**3**) 5′-ATACCTGGGGGAGTATATGTGGAGGG-3′
(**4**) 5′-GGGACGGGATAGCGGAGGAAGGTAT-3′
(**5**) 5′-HS$(CH_2)_6$TTTGGGTAGGGCGGGTTGGG-3′
(**6**) 5′-HS$(CH_2)_6$AAAAAATACCTGGGGGAGTATATGTGGA-GGG-3′
(**7**) 5′-GGGTTGGGCGGGATGGGTTACCTCAGTGCTTATT-CGAAACCCAAA $(CH_2)_6$-SH-3′
(**8**) 5′-TCGAATAAGCACTGAGGT-3′
(**9**) 5′-GGGTAGGGCGGGTTGGGCTATCATCTTGGCAATT-TATTAGCCC $(CH_2)_6$-SH-3′
(**10**) 5′-GGGTAGGGCGGGTTGGGTTCCTGGGGGAGTATT-GATAGAACCC $(CH_2)_6$-SH-3′
(**11**) 5′-ATAAATTGCCAAGATGAT-3′
(**12**) 5′-TATCAATACTCCCCCAGG-3′

Analysis of Hg^{2+} Ions and ATP by the DNAzyme Subunits. The dilution buffer solution consisted of 25 mM 4-(2-hydroxyethyl)-1-piperazinnethanesulfonic acid, HEPES, 20 mM KNO_3, 200 mM $NaNO_3$, 0.025% Triton X-100, and 1% DMSO, pH 7.4.

The reaction buffer solution consisted of 25 mM HEPES, 20 mM KNO_3, 200 mM $NaNO_3$, 0.025% Triton X-100, and 1% DMSO, pH 9.

Nucleic acids (**1**−**4**) were diluted with the above dilution buffer solution and annealed at 90 °C to yield a concentration of 1 μM. Different concentrations of Hg^{2+} or ATP were added to the annealed nucleic acid mixtures (**1**) and (**2**), or (**3**) and (**4**), respectively. The systems were allowed to incubate for 1 h at room temperature. Then, 5 μM hemin (diluted from the stock solution with the dilution buffer solution) was added and incubated for an additional 1 h at room temperature to form the G-quadruplex structure.

Measurements were made in a cuvette that included 0.25 μM G-quadruplex, 0.125 μM hemin, 0.5 mM luminol, and 30 mM H_2O_2. Briefly, 50 μL of DNAzyme solution, 200 μL of reaction buffer, and 50 μL of 5 mM luminol solution (diluted from the stock solution with the reaction buffer) were added to a cuvette sequentially. Then, 200 μL of 75 mM H_2O_2 stock solution was quickly added to the cuvette. The light emission intensity was measured immediately.

Preparation of GSH-Capped QDs. QDs were precipitated from the toluene solution by addition of 2 mL of methanol to 0.5 mL of the QDs in toluene, followed by centrifugation for 5 min at 3000 rpm. The resulting precipitate was dissolved in 1 mL of chloroform, to which was added a solution (200 μL) of a glutathione, GSH (containing 0.142 g of GSH and 40 mg of KOH in 2 mL of methanol), and the resulting mixture was shaken. After the addition of 1.5 mL of 1 mM NaOH solution in water, all particles were transferred to the water phase. The QDs solution was separated from the chloroform by centrifugation for 1 min. The excess of GSH was removed by two successive precipitation steps of QDs, using NaCl and methanol, followed by centrifugation. The resulting QDs were dissolved in 200 μL of a 10 mM HEPES buffer, pH 7.4. It should be noted that the GSH-capped QDs exhibit high stability, and they could be stored for several months without precipitation, while retaining their photophysical properties. Also, the particles are stable in the pH range of 6.3−8.8 and are not affected by the change of the buffer solution. The photoluminescence quantum yields of the CdSe/ZnS QDs before and after modification of GSH corresponded to 0.45 and 0.38 for the 620 nm QDs, 0.42 and 0.31 for the 560 nm QDs, and 0.5 and 0.35 for the 490 nm QDs. Fluorescein dye was used as a reference dye for the 490 nm QDs. Rhodamine 6G was used for all other wavelengths.

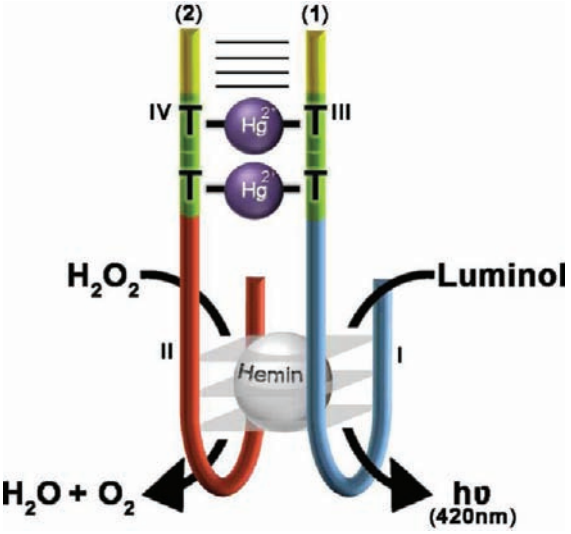

Figure 1. Chemiluminescent analysis of Hg^{2+} ions by two HRP-DNAzyme subunits containing T sites for Hg^{2+} recognition.

Preparation of Nucleic Acid-Modified CdSe/ZnS QDs. The GSH-capped QDs (1 nmol) in HEPES buffer, 200 μL, were reacted with 100 μL of an EMCS stock solution (1 mg mL^{-1}), and the mixture was shaken for 15 min. The QDs were purified by precipitation by the addition of 1 mL of methanol and 3 mg of NaCl, to remove excess of EMCS, and the QDs were redissolved in 10 mM HEPES buffer (pH 7.4). The purified QDs were reacted with the freshly reduced and purified thiolated oligonucleotides (25 μL, 100 μM), and the resulting solution was shaken for 2 h. Finally, the excess DNA was removed by precipitation of the QDs, and the purified particles were dissolved in phosphate buffer solution (100 μL, pH 7.4, 10 mM). The resulting QDs were stable for at least 6 weeks with no noticeable precipitation or change in their luminescence properties.

Determination of the Loading of the CdSe/ZnS QDs with the Oligonucleotides. The absorption spectrum of the CdSe/ZnS nanoparticles of known concentration was recorded prior to the modification of the particles. The absorption spectrum of the oligonucleotide-functionalized CdSe/ZnS QDs was, then, recorded and the spectrum was normalized to the same OD value at 450 nm observed for the nonmodified QDs. Since DNA is not absorbing at 450 nm, the subtraction of the spectrum of the oligonucleotide-functionalized QDs from the nonmodified QDs yielded the absorbance of the DNA associated with the QDs. The absorbance difference at λ = 260 nm allows the calculation of the concentration of DNA. Knowing the concentration of the QDs, the DNA/QDs ratio was, then, calculated.

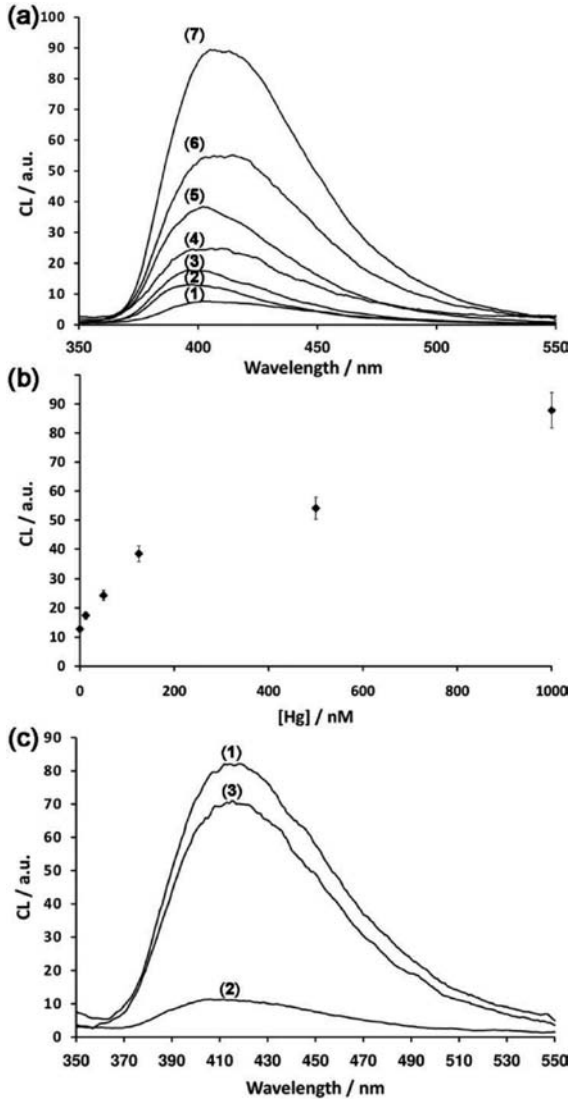

Figure 2. (a) (1) Chemiluminescence light intensity generated by hemin, 1.25×10^{-7} M; (2) chemiluminescence light intensity generated by the nucleic acids (**1**) and (**2**) (each 250 nM) in the presence of hemin, 1.25×10^{-7} M; (3−7) chemiluminescence light intensities generated by (**1**) and (**2**) in the presence of hemin and different concentrations of Hg^{2+}: (3) 1.25×10^{-8} M, (4) 5×10^{-8} M, (5) 1.25×10^{-7} M, (6) 7×10^{-7} M, (7) 1×10^{-6} M. (b) Resulting calibration curve derived from the increase in the chemiluminescence signal at λ = 402 nm. Each data point is the average of N = 5 individual measurements. The error bars indicate the standard deviation. (c) Switching of the chemiluminescent sensing of Hg^{2+} ions by the HRP-DNAzyme subunits: (1) in the presence of Hg^{2+}, 1 μM; (2) after the addition of cysteine 10 μM; (3) after the addition of Ag^{+} 20 μM to bind cysteine and release the Hg^{2+} ions.

The Analysis of ATP and DNA by the DNAzyme-Modified QDs Using CRET as the Readout Signal. *Analysis of ATP or DNA.* The (**6**)- or (**7**)-modified QDs solution (1 nM) diluted in 25 mM HEPES, 20 mM KNO_3, and 200 mM $NaNO_3$, pH 9, was incubated with different concentrations of ATP or the analyte DNA, in the presence of 100 nM (**4**), or (**8**), 1×10^{-6} M, and 10 nM hemin for 1 h. Measurement was performed after addition of 50 μM luminol and 300 μM H_2O_2. The light emission intensity was measured immediately.

Multiplexed Analysis of DNA. The mixture of (**7**), (**9**), and (**10**)-modified QDs solution (1 nM) diluted in 25 mM HEPES, 20 mM KNO_3, and 200 mM $NaNO_3$, pH 9, was incubated with 1 μM of the respective analyte DNA, and 10 nM hemin for 1 h. Measurement was performed after addition of 50 μM luminol and 300 μM H_2O_2. The light emission intensity was measured immediately.

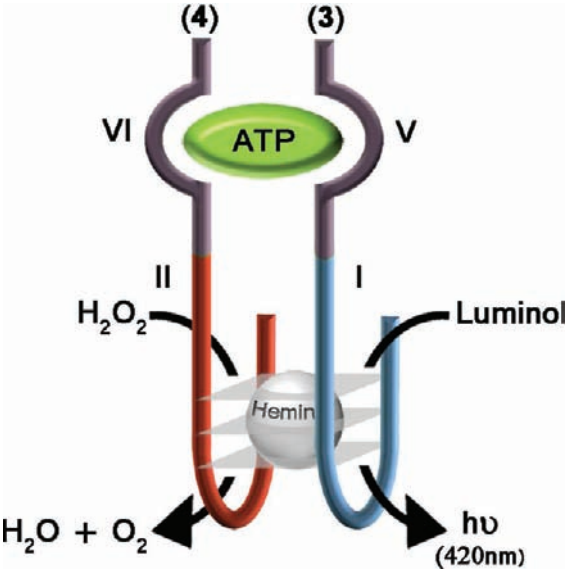

Figure 3. Chemiluminescent analysis of ATP by two subunits consisting of the conjugated anti-ATP and HRP-DNAzyme subunits.

Optical Instrumentation. Real-time fluorescence measurements were carried out using a photoncounting spectrometer (Edinburgh Instruments, FLS 920) equipped with a cooled photomultiplier detection system connected to a computer (F900 v.6.3 software, Edinburgh Instruments).

RESULTS AND DISCUSSION

Figure 1 shows the chemiluminescent method to analyze Hg^{2+} ions. The nucleic acids (**1**) and (**2**) include, each, the G-rich HRP-mimicking DNAzyme subunits I and II and the T-containing sites as Hg^{2+} recognition units in subunits III and IV, respectively. While the subunits III and IV include partial complementarities, the nucleic acids (**1**) and (**2**) do not assemble, at room temperature, into a stable catalytic hemin G-quadruplex. In the presence of Hg^{2+} ions, the respective T−Hg^{2+}−T complexes between domains III and IV are formed. The resulting duplex structure stabilizes cooperatively the formation of the hemin/G-quadruplex between (**1**) and (**2**). The assembled DNAzyme structure catalyzes the H_2O_2 oxidation of luminol, while generating chemiluminescence (λ = 420 nm). Figure 2a shows the chemiluminescence light intensities upon analyzing different concentrations of Hg^{2+}-ions, and the resulting calibration curve, Figure 2b. The detection limit for analyzing Hg^{2+} is 10 nM, a value that is comparable to the sensitivity observed upon the aggregation of Au NPs,[7] yet, it is substantially faster. The reaction of the resulting Hg^{2+}-bridged hemin/G-quadruplex with cysteine resulted in the elimination of Hg^{2+} from the nucleic acid structure, while forming the respective stable Hg^{2+}−cysteine complex. Addition of Ag^{+} ions exhibiting a higher affinity for cysteine regenerates the Hg^{2+}-bridged hemin/G-quadruplex that generates chemiluminescence. Figure 2c shows the cyclic switchable generation of the Hg^{2+}-bridged DNAzyme structure and its separation by cysteine, and the resulting "ON" and "OFF" switching of the chemiluminescence of the system. Besides the

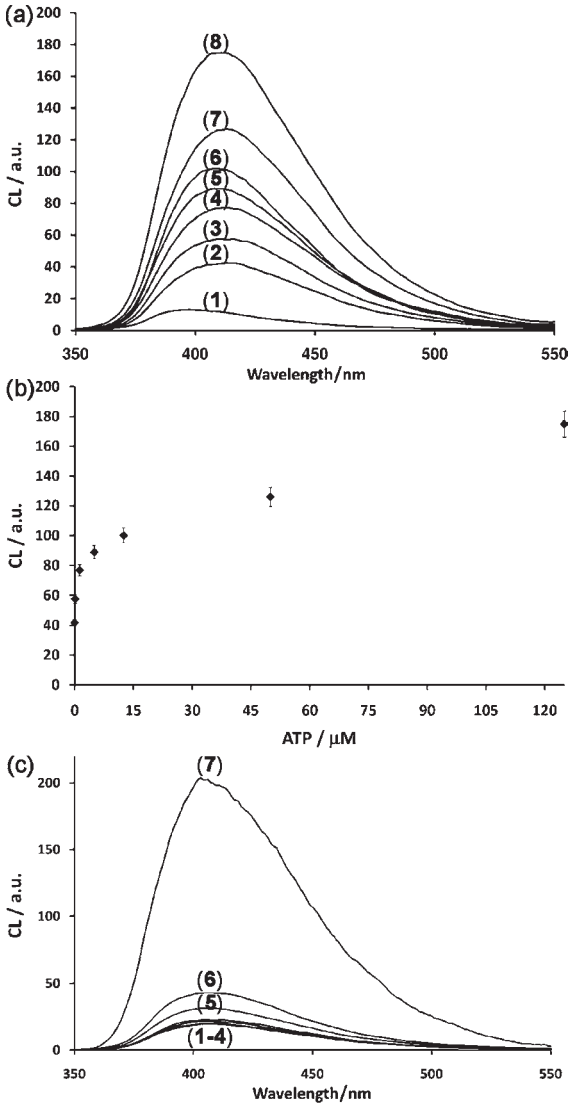

Figure 4. (a) (1) Chemiluminescence light intensity generated by hemin, 1.25×10^{-7} M; (2) chemiluminescence light intensity generated by the nucleic acids (**3**) and (**4**) (each 250 nM) in the presence of hemin, 1.25×10^{-7} M; (3−8) chemiluminescence light intensities generated by (**3**) and (**4**) in the presence of hemin and variable concentrations of ATP: (3) 1.25×10^{-7} M, (4) 1.25×10^{-6} M, (5) 5×10^{-6} M, (6) 1.25×10^{-5} M, (7) 5×10^{-5} M, (8) 1.25×10^{-4} M. (b) Resulting calibration curve derived from the increase in the chemiluminescence signal at $\lambda = 410$ nm. Each data point is the average of $N = 5$ individual measurements. The error bars indicate the standard deviation. (c) (1) Chemiluminescence light intensity generated by the nucleic acids (**3**) and (**4**) (each 250 nM) in the presence of hemin, 1.25×10^{-7} M; (2−7) chemiluminescence light intensities generated by (**3**) and (**4**) in the presence of hemin and (2) GTP, 5×10^{-4} M, (3) CTP, 5×10^{-4} M, (4) UTP, 5×10^{-4} M, (5) ADP, 5×10^{-4} M, (6) AMP, 5×10^{-4} M, (7) ATP, 5×10^{-4} M.

demonstration of an ion-stimulated chemiluminescent switch, the system reveals the recycling of the sensing subunits upon the addition of cysteine.

The similar concept was applied to develop a chemiluminescent ATP aptasensor, Figure 3. The nucleic acids (**3**) and (**4**) were used as two nucleic acid subunits. While (**3**) and (**4**) include the domains I and II of the HRP-mimicking DNAzyme, the

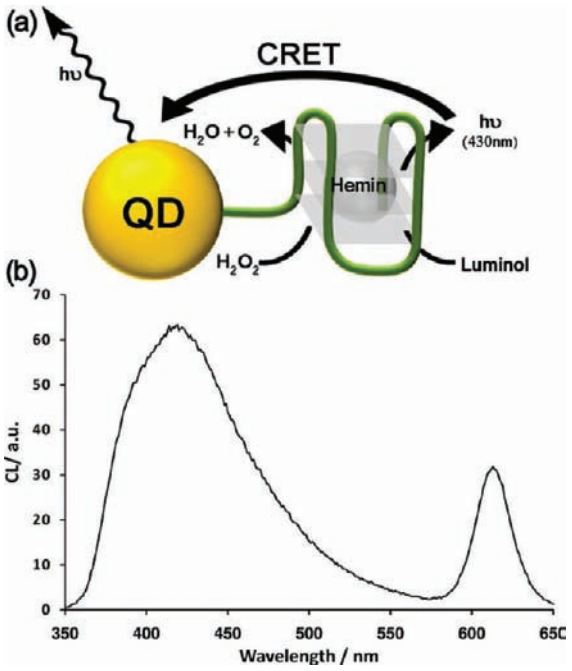

Figure 5. (a) The hemin−G-quadruplex/QD conjugate and the CRET process proceeding in the presence of hemin, luminol, and H_2O_2. (Note that the QD is modified by ca. 9 nucleic acids.) (b) Luminescence spectrum corresponding to the CRET-generated luminescence of the QDs at $\lambda = 612$ nm.

domains V and VI consist of the anti-ATP aptamer. In the absence of ATP, the subunits (**3**) and (**4**) lack the stability to assemble the active hemin/G-quadruplex, but in the presence of ATP, the aptamer subunits−ATP complex cooperatively stabilizes the hemin/G-quadruplex. This leads to the generation of chemiluminescence as a result of the DNAzyme catalyzed oxidation of luminol. Figure 4a depicts the chemiluminescence intensities upon analyzing different concentrations of ATP. As the concentration of ATP increases, the chemiluminescence signals are intensified, consistent with the higher content of the active DNAzyme. Figure 4b shows the derived calibration curve. This method enabled the detection of ATP with a sensitivity that corresponds to 100 nM. The sensing of ATP is specific and the interaction of (**3**) and (**4**) in the presence of adenosine monophosphate, AMP, or adenosine diphosphate, ADP, yielded low chemiluminescence signals close to the background chemiluminescence of the system. Furthermore, guanosine 5′-triphosphate, GTP, cytidine 5′-triphosphate, CTP, and uridine 5′-triphosphate, UTP, demonstrated no affinity for the aptamer subunits, leading to the background chemiluminescence signal of the system in the absence of any analyte, as demonstrated in Figure 4c.

The analytical platforms using chemiluminescence as a readout signal suffer, however, from the fact that hemin itself acts as a catalyst, albeit inefficient, for the oxidation of luminol by H_2O_2, and the generation of chemiluminescence. This leads to relatively high background signals. To overcome this limitation, we have conjugated the hemin/G-quadruplex with CdSe/ZnS quantum dots (QDs) with the goal that a chemiluminescence resonance energy transfer (CRET) process triggers-on the luminescence of the QDs. As the CRET process is dominated by the intimate short distance between the chemiluminescent light source and the QDs, the chemiluminescence of diffusional hemin should not

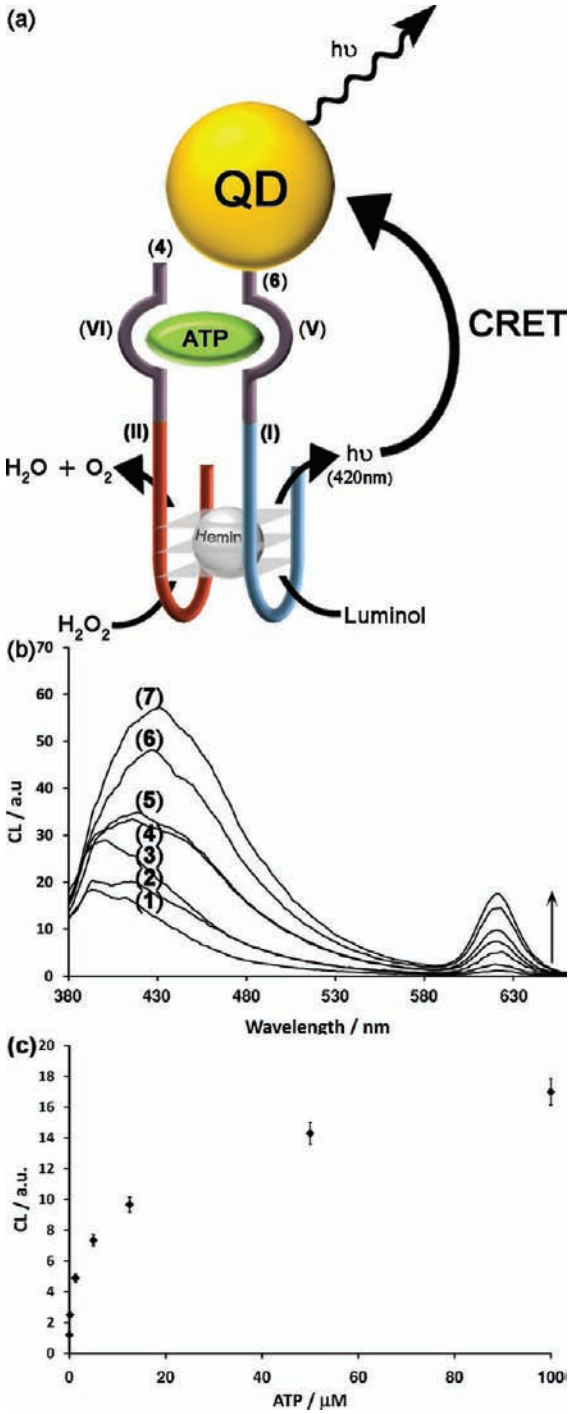

Figure 6. (a) Analysis of ATP through the CRET from luminol, oxidized by the assembled hemin−G-quadruplex, to the QDs. (Note that the QD is modified by ca. 10 nucleic acids.) (b) Luminescence spectrum corresponding to the CRET signal of the QDs at $\lambda = 612$ nm in the absence of ATP, curve (1), and in the presence of different concentrations of ATP: (2) 1.25×10^{-7} M, (3) 1.25×10^{-6} M, (4) 5×10^{-6} M, (5) 12.5×10^{-6} M, (6) 5×10^{-5} M, (7) 1×10^{-4} M, (c) Calibration curve corresponding to the increase in the CRET signal at $\lambda = 620$ nm. Each data point is the average of $N = 5$ individual measurements. The error bars indicate the standard deviation.

affect the luminescence of the QDs. While the CRET process was previously observed between luminol and horseradish peroxidase-conjugated QDs,[38] the process was never implemented for analytical applications, and DNAzyme-stimulated CRET was not demonstrated yet. In addition, the use of the HRP-mimicking DNAzyme as a CRET generator paves the way to develop versatile sensing platforms involving nucleic acid-functionalized QDs as CRET acceptors. Semiconductor QDs have been previously employed and studied as energy acceptors in processes, such as bioluminescence resonance energy transfer,[39,40] BRET; however, their applications as CRET acceptors are still scarce.[41,42] The CRET process requires a spectral overlap between a chemiluminescent donor (e.g., luminol $\lambda_{CL} = 420$ nm) and the absorption of the acceptor QDs in order for an energy transfer to occur. Accordingly, Figure 5a illustrates the schematic configuration of the CRET system. The CdSe/ZnS QDs ($\lambda_{em} = 620$ nm) were modified with a glutathione (GSH) capping layer and were covalently linked to the thiolated nucleic acid (**5**) that includes the G-quadruplex sequence. Spectroscopic analysis of the (**5**)-functionalized QDs indicated that approximately 9 units of (**5**) were associated with each particle. (For the detailed synthesis and characterization of the modified QDs, see the Experimental Section.) In the presence of hemin, luminol, and hydrogen peroxide, the HRP-mimicking DNAzyme catalyzed the oxidation of luminol by H_2O_2, resulting in the CRET between luminol and the DNAzyme−QD bioconjugates, as shown in Figure 5b. The CRET efficiency was determined according to the literature method[41] to be ca. 15% by dividing the integral area of the QDs emission spectrum by the integral area of the whole spectrum of the luminol−QDs conjugate. The effective CRET signal is attributed to the fact that the DNAzyme linked to the QDs surface can continuously catalyze the luminol/hydrogen peroxide chemiluminesence reaction, and the close proximity of the light source to the QDs leads to an effective CRET. One should note, however, that the chemiluminescence intensity is changed during the different experiments due to the evolution of the catalytic hemin/G-quadruplexes. Furthermore, since the hemin/G-quadruplex also quenches the luminescence of the QDs via electron transfer,[35] the CRET efficiency is slightly altered in the different experiments. Knowing the CRET efficiency, and estimating the geometrical separation between the QDs and the G-quadruplex, we estimated the Förster radius to be in the range of 3−3.5 nm ($E = R_0^6/(R_0^6 + R^6)$, where E is the CRET efficiency, and R and R_0 correspond to the geometrical distance separating the QDs and G-quadruplex and the Förster distance, respectively).

The ability to trigger on the luminescence of the DNAzyme-functionalized QDs by luminol enabled the use of the conjugates as luminescent probes for the analysis of aptamer−substrate complexes. Figure 6 depicts the CRET-based analysis of ATP by the hemin/G-quadruplex conjugated aptasensor. GSH-capped CdSe/ZnS QDs ($\lambda_{em} = 620$ nm) were covalently tethered to the thiol-functionalized nucleic acid (**6**) (average loading ca. 10 units per particle. See the Experimental Section). The nucleic acid (**6**) consists of the anti-ATP aptamer subunit, (V), and the HRP-mimicking DNAzyme subunit, (I). Treatment of the (**6**)-functionalized QDs with ATP in the presence of the nucleic acid (**4**) that includes the complementary aptamer subunit, region (VI), and the second DNAzyme subunit (II) resulted in the formation of the ATP hemin/G-quadruplex-QDs complex. Figure 6b shows that, upon the addition of ATP, the resulting chemiluminescence stimulates a CRET process, evident by the luminescence of the QDs, $\lambda_{em} = 620$ nm. As the concentration of ATP increases, the CRET signals are intensified, due to the

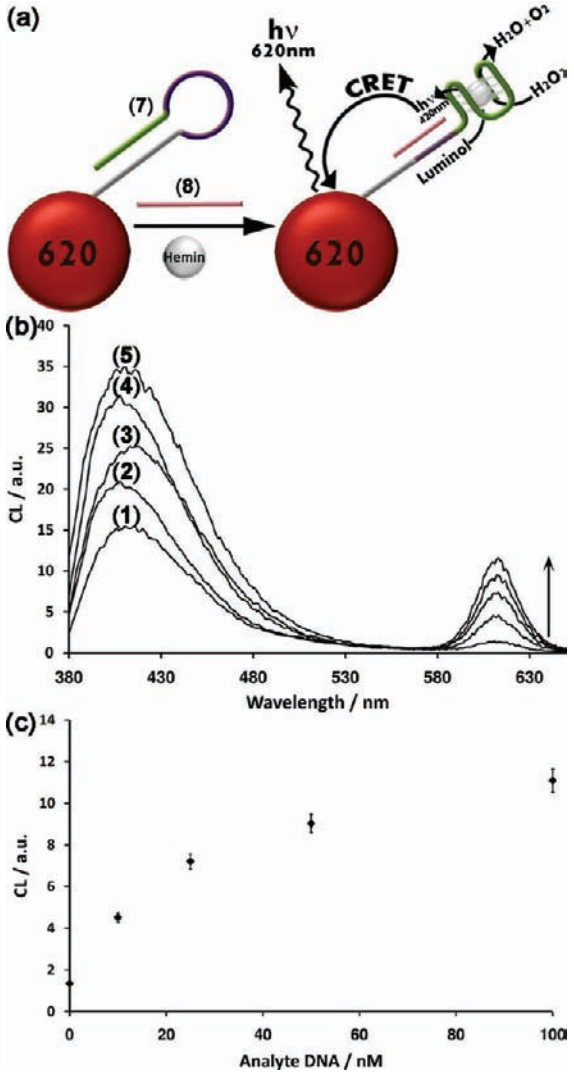

Figure 7. (a) Analysis of target DNA through the CRET process from luminol, oxidized by the assembled hemin−G-quadruplex, to the QDs. (Note that the QD is modified by ca. 10 nucleic acids.) (b) Luminescence spectrum corresponding to the CRET signal of the QDs at λ = 620 nm in the absence of (**8**), curve (1), and in the presence of different concentrations of (**8**): (2) 10 nM, (3) 25 nM, (4) 50 nM, (5) 100 nM . (c) Calibration curve corresponding to the increase in the CRET signal at λ = 610 nm. Each data point is the average of N = 5 individual measurements. The error bars indicate the standard deviation.

higher chemiluminescence signals. Control experiments revealed that no CRET signal was detected in the absence of ATP, implying that the low-intensity chemiluminescence generated by diffusional hemin does not yield a significant CRET. Figure 6c shows the resulting calibration curve. ATP could be detected with a sensitivity corresponding to 100 nM. While the sensitivity is comparable to that observed for the chemiluminescent detection of ATP by the two base subunits, the advantage of the CRET-based sensor is the lack of a background chemiluminescence signal.

The CRET process was further implemented to analyze DNA, Figure 7. The glutathione-capped CdSe/ZnS QDs (λ_{em} = 620 nm) were functionalized with the thiol-modified nucleic acid hairpin structure, (**7**) (average loading of ca. 10 units per particle). The HRP-mimicking DNAzyme sequence is blocked in

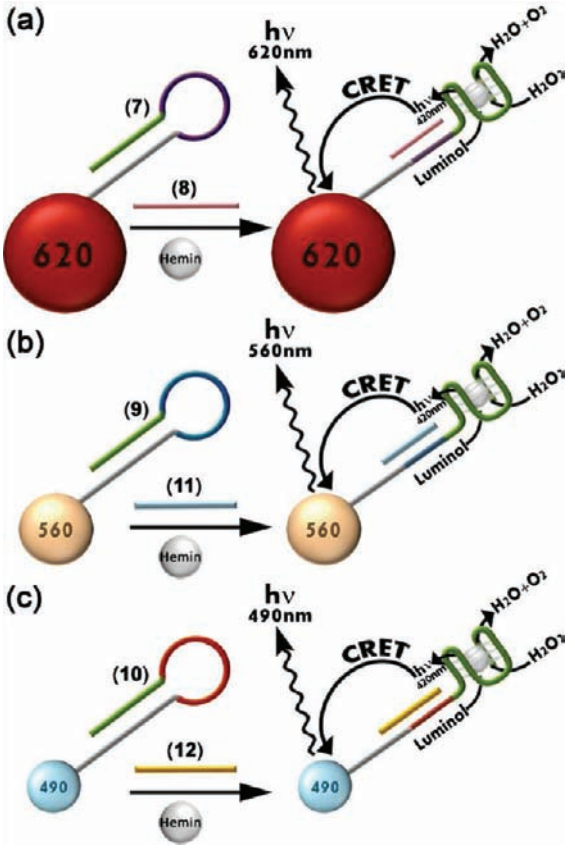

Figure 8. Multiplexed analysis of the different target DNAs using three different sized CdSe/ZnS QDs emitting at (a) 620 nm, (b) 560 nm, and (c) 490 nm, using the CRET sensing platform.

the stem duplex structure of the hairpin. The loop region of the hairpin includes the recognition sequence for the analyte DNA, (**8**). In the presence of the analyte DNA, the hairpin structure opens, resulting in the self-assembly of the hemin/G-quadruplex DNAzyme. The resulting chemiluminescence stimulates the CRET process and triggers-on the luminescence of the QDs. Figure 7b depicts the CRET signals and the resulting calibration curve, Figure 7c. As the concentration of (**8**) increases, the CRET signals are higher, consistent with the higher content of active DNAzyme in the system. The sensitivity for the detection of the analyte DNA by the CRET process corresponds to 1×10^{-8} M. This sensitivity is comparable to other QDs-based FRET sensing platforms[43,44] (1×10^{-8} to 1×10^{-9} M). Nonetheless, the lack of a high background signal and the multiplexed analysis of DNA by the CRET sensing platform (vide infra) demonstrate the advantage of our method. Realizing that different sized QDs may be excited by the chemiluminescence wavelength generated by luminol, the sensing platform was further implemented for the multiplexed analysis of three different DNAs, Figure 8. Three different sized CdSe/ZnS QDs (λ_{em} = 490 nm, λ_{em} = 560 nm, λ_{em} = 620 nm) were modified with the hairpin structures (**7**), (**9**), and (**10**); each of these hairpin structures includes in the duplex stem structure the blocked HRP-mimicking DNAzyme sequence, while the loop regions of (**7**), (**9**), and (**10**) are complementary to the DNA analytes (**8**), (**11**), and (**12**), respectively. As the chemiluminescence generated by the hemin/G-quadruplex is capable to stimulate the CRET to any of these QDs, the opening of any hairpin by the

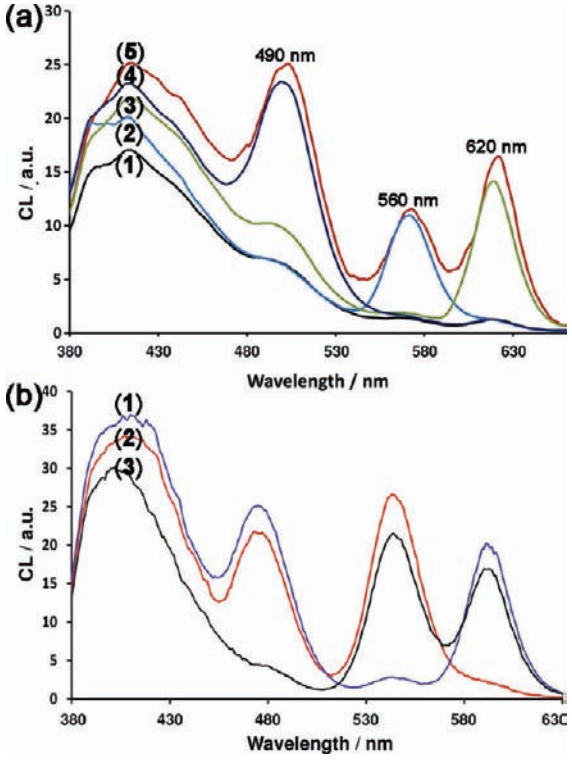

Figure 9. (a) (1) The luminescence spectrum in the presence of the QDs mixture corresponding to the CRET signal in the absence of the different DNA targets; (2) in the presence of the QDs mixture and (**11**); (3) in the presence of the QDs mixture and (**8**); (4) in the presence of the QDs mixture and (**12**); (5) in the presence of the QDs mixture and all three targets (**8**), (**11**), and (**12**). (b) The luminescence spectrum in the presence of the QDs mixture corresponding to the CRET signal in the presence of (**8**) and (**12**), curve (1), (**11**) and (**12**), curve (2), and (**8**) and (**11**), curve (3).

respective analyte will result in the chemiluminescence generation by the hemin/G-quadruplex, and the consequent triggering of the luminescence of the adjacent QDs. Figure 9a shows the luminescence features of the mixture of the three different sized QDs modified with hairpins (**7**), (**9**), and (**10**) after interaction with the DNA analytes (**8**), (**11**), and (**12**), in the presence of hemin and H_2O_2/luminol. The interaction of the QDs mixture with (**8**) triggers the luminescence of the 620 nm luminescent QDs, consistent with the selective opening of hairpin (**7**) and the formation of the hemin/G-quadruplex. Similarly, the treatment of the modified-QDs mixture with the analytes (**11**) or (**12**) triggers the luminescence of the 560 or 490 nm luminescent QDs, respectively. This is consistent with the selective opening of hairpins (**9**) or (**10**), respectively. In turn, treatment of the QDs mixture with all three analytes, (**8**), (**11**), and (**12**), results in the CRET emission of all three sized QDs at 490, 560, and 620 nm. Also, the interaction of the QDs mixture in the presence of different combinations of two target DNAs leads to the CRET signals from the respective QDs, as can be seen in Figure 9b. These results demonstrate the multiplexed parallel analysis of all three target DNAs by the CRET process.

CONCLUSIONS

The present study has demonstrated the application of self-assembled hemin/G-quadruplex nanostructures for the chemiluminescence resonance energy transfer detection of aptamer−substrate complexes, metal ions (Hg^{2+}), and DNA. Particularly important is the use of the CRET process between the chemiluminescence source and the QDs as a readout signal for the sensing events. The confinement of the CRET reaction to the hemin/G-quadruplex DNAzyme−QDs conjugates leads to several advantages: (i) Exclusion of chemiluminescent background signals due to diffusional hemin; and (ii) possibilities to perform multiplex analyses with different sized QDs and of variable compositions using a common internal light source, generated by the recognition events. Several future goals will involve the fundamental correlation between the CRET efficiency and the distance separating the QDs and the DNAzyme, and the application of the CRET process to follow biocatalytic transformations.

AUTHOR INFORMATION

Corresponding Author
willnea@vms.huji.ac.il

Author Contributions
[†]These authors contributed equally.

ACKNOWLEDGMENT

This research is supported by the EC NANOGNOSTICS research project.

REFERENCES

(1) Elghanian, R.; Storhoff, J. J.; Mucic, R. C.; Letsinger, R. L.; Mirkin, C. A. *Science* **1997**, *277*, 1078–1081.
(2) Liu, J. W.; Lu, Y. *Angew. Chem., Int. Ed.* **2006**, *45*, 90–94.
(3) Liu, J. W.; Lu, Y. *Anal. Chem.* **2004**, *76*, 1627–1632.
(4) Liu, J.; Mazumdar, D.; Lu, Y. *Angew. Chem., Int. Ed.* **2006**, *45*, 7955–7959.
(5) Lin, Y. W.; Huang, C. C.; Chang, H. T. *Analyst* **2011**, *136*, 863–871.
(6) Liu, J. W.; Lu, Y. *J. Am. Chem. Soc.* **2004**, *126*, 12298–12305.
(7) Li, D.; Wieckowska, A.; Willner, I. *Angew. Chem. Int. Ed.* **2008**, *47*, 3927–3931.
(8) Yang, Y.; Zhao, L. *Trends Anal. Chem.* **2010**, *29*, 980–1003.
(9) Tombelli, S.; Minunni, M.; Mascini, M. *Biosens. Bioelectron.* **2005**, *20*, 2424–2434.
(10) Navani, N. K.; Li, Y. *Curr. Opin. Chem. Biol.* **2006**, *10*, 272–281.
(11) Asano, A.; Sullivan, C. M.; Yanagisawa, A.; Kimoto, H.; Kurotsu, T. *Anal. Bioanal. Chem.* **2002**, *372*, 44–48.
(12) Ho, H. A.; Leclerc, M. *J. Am. Chem. Soc.* **2004**, *126*, 1384–1387.
(13) Kirby, R.; Cho, E. J.; Gehrke, B.; Bayer, T.; Park, Y. S.; Neikirk, D. P.; McDevitt, J. T.; Ellington, A. D. *Anal. Chem.* **2004**, *76*, 4066–4075.
(14) Peng, H.; Zhang, L. J.; Kjallman, T. H. M.; Soeller, C.; Travas-Sejdic, J. *J. Am. Chem. Soc.* **2007**, *129*, 3048–3049.
(15) Jiang, G.; Susha, A. S.; Lutich, A. A.; Stefani, F. D.; Feldmann, J.; Rogach, A. L. *ACS Nano* **2009**, *3*, 4127–4131.
(16) Patolsky, F.; Gill, R.; Weizmann, Y.; Mokari, T.; Banin, U.; Willner, I. *J. Am. Chem. Soc.* **2003**, *125*, 13918–13919.
(17) Levy, M.; Cater, S. F.; Ellington, A. D. *ChemBioChem* **2005**, *6*, 2163–2166.
(18) Freeman, R.; Li, Y.; Tel-Vered, R.; Sharon, E.; Elbaz, J.; Willner, I. *Analyst* **2009**, *134*, 653–656.
(19) Willner, I.; Shlyahovsky, B.; Zayats, M.; Willner, B. *Chem. Soc. Rev.* **2008**, *37*, 1153–1165.
(20) Liu, J.; Lu, Y. *Anal. Chem.* **2003**, *75*, 6666–6672.
(21) Liu, J.; Lu, Y. *J. Am. Chem. Soc.* **2007**, *129*, 9838–9839.
(22) Moshe, M.; Elbaz, J.; Willner, I. *Nano Lett.* **2009**, *9*, 1196–1200.

(23) Liu, J.; Lu, Y. *J. Am. Chem. Soc.* **2004**, *126*, 12298–12305.
(24) Travascio, P.; Li, Y.; Sen, D. *Chem. Biol.* **1998**, *5*, 505–517.
(25) Travascio, P.; Bennet, A. J.; Wang, D. Y.; Sen, D. *Chem. Biol.* **1999**, *6*, 779–787.
(26) Xiao, Y.; Pavlov, V.; Niazov, T.; Dishon, A.; Kotler, M.; Willner, I. *J. Am. Chem. Soc.* **2004**, *126*, 7430–7431.
(27) Teller, C.; Shimron, S.; Willner, I. *Anal. Chem.* **2009**, *81*, 9114–9119.
(28) Lu, N.; Shao, C.; Deng, Z. *Chem. Commun.* **2008**, 6161–6163.
(29) Li, D.; Shlyahovsky, B.; Elbaz, J.; Willner, I. *J. Am. Chem. Soc.* **2007**, *129*, 5804–5805.
(30) Li, T.; Li., B.; Wang, E.; Dong, S. *Chem. Commun.* **2009**, 3551–3553.
(31) Liu, J.; Lu, Y. *Angew. Chem. Int. Ed.* **2007**, *46*, 7587–7590.
(32) Cheglakov, Z.; Weizmann, Y.; Basnar, B.; Willner, I. *Org. Biomol. Chem.* **2007**, *5*, 223–225.
(33) Bi, S.; Li, L.; Zhang, S. *Anal. Chem.* **2010**, *82*, 9447–9454.
(34) Zhu, C.; Wen, Y.; Li, D.; Wang, L.; Song, S.; Fan, C.; Willner, I. *Chem.—Eur. J.* **2009**, *15*, 11898–11903.
(35) Sharon, E.; Freeman, R.; Willner, I. *Anal. Chem.* **2010**, *82*, 7073–7077.
(36) Xiao, Y.; Pavlov, V.; Gill, R.; Bourenko, T.; Willner, I. *ChemBioChem* **2004**, *5*, 374–379.
(37) Bi, S.; Zhang, J.; Zhang, S. *Chem. Commun.* **2010**, *46*, 5509–5511.
(38) Huang, X.; Li, L.; Qian, H.; Dong, C.; Ren, J. *Angew. Chem., Int. Ed.* **2006**, *45*, 5140–5143.
(39) So, M. K.; Xu, C. J.; Loening, A. M.; Gambhir, S. S.; Rao, J. H. *Nat. Biotechnol.* **2006**, *24*, 339–343.
(40) Yao, H.; Zhang, Y.; Xiao, F.; Xia, Z.; Rao, J. *Angew. Chem., Int. Ed.* **2007**, *46*, 4346–4349.
(41) Li, Z.; Wang, Y.; Zhang, G.; Xu, W.; Han, Y. *J. Lumin.* **2010**, *30*, 995–999.
(42) Wang, H. Q.; Li, Y. Q.; Wang, J. H.; Xu, Q.; Li, X. Q.; Zhao, Y. D. *Anal. Chim. Acta* **2008**, *610*, 68–73.
(43) Kim, J. H.; Chaudhary, S.; Ozkan, M. *Nanotechnology* **2007**, *18*, 195105.
(44) Cady, N. C.; Strickland, A. D.; Batt, C. A. *Mol. Cell. Probes* **2007**, *21*, 116–124.